Modulation of Structure and Dynamics of Water Under Alternating Electric Field and the Role of Hydrogen Bonding

M. Shafiei, N. Ojaghlou, S. Zamfir, D. Bratko*, and A. Luzar

Department of Chemistry, Virginia Commonwealth University, Richmond, Virginia 23284, United States

Abstract

Using Molecular Dynamics simulations, we investigate the effect of alternating (AC) electric field on static and dynamic properties of water. The central question we address is how hydrogen bonds respond to perpetual field-induced dipole reorientations. We assess structural perturbations of water network and changes of hydrogen bond dynamics in a range of alternating electric field strengths and frequencies using a non-polarizable water model, SPC/E, and two distinct polarizable models: SWM4-NDP and BK3. We confirm that AC field causes only moderate structural perturbations. Dynamic properties, including the rates of bond breaking, switching of hydrogen-bonding partners, and diffusion, accelerate with the strength of AC fields. All models reveal a nonmonotonic frequency dependence with fastest dynamics at frequencies around 200 GHz where the period of the field oscillation is commensurate with the average time it takes a typical proton to switch from one acceptor to another. Higher frequencies result in smaller amplitudes of angle oscillations and in reduced probability to complete the switch to another acceptor before the field reversal restores the original configuration. As frequency increases, these effects gradually weaken the influence of the field on the kinetics of hydrogen bonding and the associated rates of translational and rotational diffusion in water.

Keywords: oscillatory field, hydrogen bond dynamics, switching between proton acceptors, anisotropic diffusion, nonmonotonic frequency dependence

*dbratko@vcu.edu

1. Introduction

The change of the properties of water under alternating electric fields has been the subject of many experimental and modeling studies motivated by considerable applications of the phenomenon in science and technology.[1-5] Alternating Electric fields in the form of electromagnetic waves warm food in microwaves[6] in a process termed dielectric heating[7]. The alternating E-field enhances the mobility of water molecules[8] and can be used to improve water transport across different interfaces.[9] If the media contains charged particles like proteins, the alternating E-field can be used to control the diffusion of such particles[10]. The structure and dynamics of water in and around confinements including planar surfaces[11-13], nanofibers[14], or nanochannels[15] can acquire a particularly rich behavior under concerted effects of the electric field and the confinement and especially so if we apply alternating E-field.[16] English and Waldon have discussed main fundamental effects of alternating fields on water and their role in a variety of applications.[17]

In the present study, we focus on the influence of alternating (AC) electric field on water properties associated with the coupling between the field-induced alignment and hydrogen bonding. In the liquid state, water molecules participate in multiple hydrogen bonds (H-bonds). At room temperature, an average molecule has around 3.6 bonds[18] arranged according to an approximately tetrahedral coordination.[19] The H-bonding of water molecules is highly dynamic, with average bond survival of a few picoseconds.[19,20] A water molecule has a net dipole moment (experiment: 2.95 D,[21] SPC/E: 2.35 D[22], BK3: 2.64 D[23], SWM4-NDP: 2.461 D[24]), and the application of an external electric field, $\vec{\boldsymbol{E}}$, imposes a torque, $\vec{\boldsymbol{\tau}}$, on the water dipole moment $\vec{\mu}$ to align it with the field direction:

$$\vec{\boldsymbol{\tau}} = \vec{\mu} \times \vec{\boldsymbol{E}} \qquad [1]$$

Exposure of molecules to external electric fields has been studied in different situations, including the passing of an electromagnetic wave[21], electric field acting on hydration molecules around ions,[25] and external fields on water molecules inside nano-tubes[26] or next to nano-surfaces.[27] In view of the association between the alternating electric current (AC) and the alternating electric field inside a capacitor, in this paper, we interchangeably describe alternating external electric field as AC-fields or alternating E-fields. Our study pays particular attention to the effect of alternating E-fields on the H-bond dynamics of bulk water. We simulate bulk water under a sinusoidal one dimensional electric field:

$$E = E_0 \sin(2\pi\nu t)\, \hat{z} \qquad [2]$$

where E_0 is the amplitude of the E-field, ν is the frequency of the field, t is the time, and $\hat{z}$ a unit vector along the z-axis of the laboratory frame. We consider field strengths E_0 of up to 0.2 V Å^{-1}, thus avoiding the proximity of the dissociation threshold of ~0.3 V Å^{-1} estimated from the first principles calculations,[28,29] and the range of frequencies below 1000 GHz ($10\,ps < \nu^{-1} < 1\,ps$) since studying faster frequencies requires accounting for intra-molecular vibrations, which is not possible using classical molecular dynamics simulation. The above frequencies are, however, sufficient to probe the picosecond time scales of hydrogen bonding events. The wide

range of amplitudes E_0 we use to amplify the simulated field effects is comparable to field strength in the vicinity of ions[30], liquid crystals[31], ionic colloids[32] or polyelectrolytes[33], and about an order of magnitude weaker than the transient local fields associated with thermal fluctuations in liquid water[34].

Before addressing the dynamics of water molecules, we study the structure of water under the alternating E-fields by monitoring the radial distribution functions[35-37] and the oxygen-triplet tetrahedral order parameter[38,39]. We find that the structural changes are not substantial which is in agreement with previous studies.[36,40] We assess the effects of AC-E-field on hydrogen bond dynamics by using the tagged molecular pair model (TP) of Luzar and Chandler[41] along with the concept of hydrogen bond switching[42,43] that we incorporate in a modified version of Chandler and Luzar's model[44] as detailed in Section 3.2. Our results reveal considerable effects of alternating E-fields on hydrogen bond dynamics. We quantify the changes in terms of breaking and reforming rate constants and rates of proton switching between adjacent acceptors. Finally, we characterize translational and rotational rates for water molecules under alternating E-fields. Our results show a considerable anisotropy of both dynamics while also revealing an interesting nonmonotonic dependence on the AC field frequency of both translational and rotational diffusion. We show the rates of these dynamics to be correlated with characteristic times of H-bond breaking and switching events thus explaining the maximal rates of these dynamics at frequencies close to 200 GHz.[45]

2. Models and Methods

2.1. Force field

A series of Molecular Dynamics (MD) simulations were performed using three rigid models of water[46]: the non-polarizable extended simple-point charge model (SPC/E)[22,23], and two polarizable models, BK3[23], and SWM4-NDP[24]. The SPC/E model carries three fixed-point charges, while the polarizable models contain mobile charges. The SWM4-NDP is a four site polarizable water model with five total point charges including a charge on a spring attached to the oxygen atom (a classical Drude oscillator)[24]. BK3, also, has four interaction sites, but only 3 total charges which are modeled via the Gaussian-charge-on-spring.[23] SPC/E and SWM4-NDP models use the Lennard-Jones potential while BK3 employs the Buckingham potential for the short range interactions. Detailed descriptions and parameterizations can be found in the original papers[22-24].

As we showed in previous work[44], the polarizability α of the BK3 model increases with the strength of static electric field E. In this study, we add the calculation of the BK3 dipole fluctuations along the three main axes of the molecule, along the molecular bisector, $\langle \delta\mu_z^2 \rangle$, between hydrogens (in-plane fluctuations), $\langle \delta\mu_x^2 \rangle$, and out-of-plane, $\langle \delta\mu_y^2 \rangle$. The fluctuation formula for the polarizability along axis β, $\alpha_{\beta\beta} = < \delta\mu_\beta^2 > / k_B T$, enables a comparison between the polarizability tensor components at varied electric fields. The fluctuations show a considerable anisotropy, *e.g.* at E=0.2 V Å^{-1}, $\langle \delta\mu_x^2 \rangle$ = 0.018 D^2, $\langle \delta\mu_y^2 \rangle$ = 0.043 D^2, $\langle \delta\mu_z^2 \rangle$ = 0.022 D^2. For complete results see Supplementary Information.

2.2. Simulation

SPC/E and SWM4-NDP simulations were performed using Large-Scale Atomic/Molecular Massively Parallel Simulator (LAMMPS).[47] The BK3 simulations were carried out using a modified Groningen Machine for Chemical Simulations (GROMACS) [48] adapted by Marcello-Sega[49] to enable the use of Gaussian charge distributions.

Our simulation is a cubic box of size 24.85 Å containing 512 water molecules at density 0.998 g cm^{-3}. The simulation timestep is 1 fs, and the same time step is used in calculations of the H-bond correlation functions.

Periodic boundary conditions were employed in all three directions. The cutoff distance of 12 Å was used for nonelectrostatic interactions and for the shielded real-space electrostatics. We calculate long range electrostatic interactions using the particle−particle−particle−mesh (PPPM) solver[50] with 10^{-5} accuracy for SPC/E and 10^{-3} for BK3 and SWM4-NDP models. The tin foil electric boundary conditions[12] are used to offset the reduction of the applied field through dielectric screening, hence the average field remains equal to the nominal one.

By perpetually changing the direction of the external electric field, we are continuously adding energy into the system. The temperature is held constant by using non-equilibrium molecular dynamics (NEMD).[51,17]. As the dynamic variables, we study strongly depend on the temperature, comparisons of the results under different electric field strengths require the same temperature for all systems. This is achieved by the use of the Nose-Hoover thermostat thermostat[52] (T = 300 K) with a relaxation time of 0.03 ps to enable the use at high frequency fields. To examine the possible dependence of the results on the thermostatting technique, several calculations were repeated using the Velocity Rescaling (CSVR) thermostat[53], which is similar to Berendsen thermostat,[54] but rescales velocities randomly with a Gaussian probability. The relaxation time for CSVR thermostat is also 0.03 ps and we confirm there were essentially no differences between the results from the two distinct thermostats. We start sampling trajectories after a 300 ps interval to achieve a steady state when the AC field is applied and the results are averaged over another 500 ps of simulation time.

3. Results and Discussion

3.1. Structure

The direction of the alternating electric field changes twice during each period $T=1/\nu$, and each reversal of the field can lead to a partial reorientation of the water molecules. However, since hydrogen bonds (H-bonds) are directional, the rotations a water molecule interfere with existing H-bonds, breaking some of them and replacing them by new ones. To determine the effect of alternating electric field on water, we explore to what extent water molecules follow the oscialltions of the field, how this affects the H-bond network, and what are the concomitant rates of H-bond breaking and reforming.

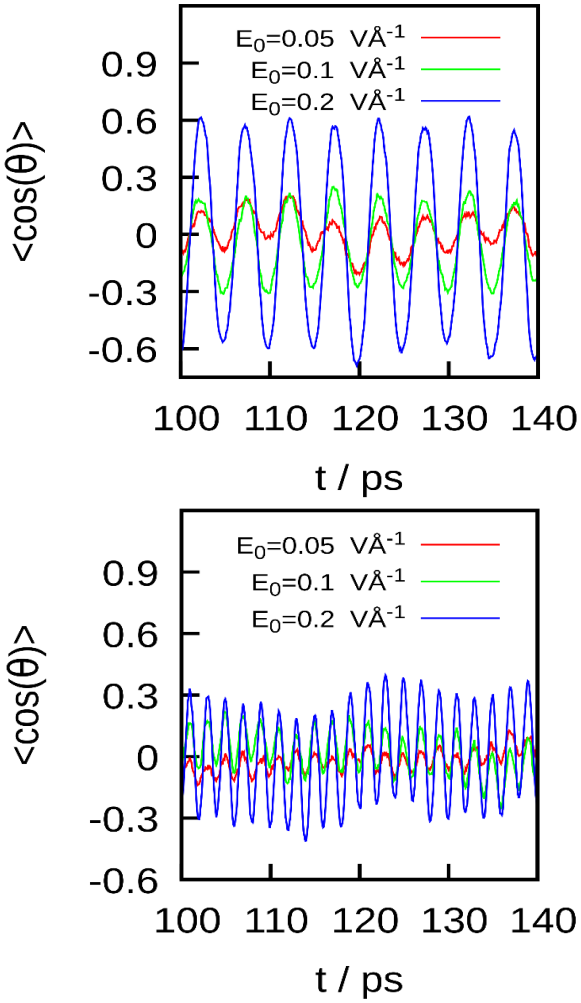

Figure 1. The average alignment of water molecules < cos(θ) > where is the angle of the water dipole moment with the field direction at three field strengths and two frequencies: 200 GHz (top) and 500 GHz (bottom). When the field is sufficiently strong, on average, water molecules follow the field even at the increased frequencies but the amplitude decreases with ν.

3.1.1. Molecular alignment

Figure 1 illustrates the time dependence of the average dipole alignment of water molecules along the *z*-axis, *i.e.* the direction of the alternating E-field:

$$\overrightarrow{\mu_z} = \frac{1}{\mathrm{N}} \sum_{all\ molecules} \vec{\mu}_z \qquad [3]$$

where $\overrightarrow{\mu_z} = \mu \cos\theta$ is the $\hat{z}$ component of a single molecule's dipole moment, $\overrightarrow{\mu_z}$ is the net dipole moment of the bulk system along the $\hat{z}$ direction, and N is the number of molecules. We see that for field strengths stronger than 0.1 V Å^{-1}, the overall system follows the field oscillations. We note that even though the average orientation of water molecules, $< cos\theta >$ where θ is the angle between the dipole moment vector, μ, and the direction of the field, follows the E-field, not

all the water molecules are actually aligned with the field.[55] The reorientation with the field oscillation is a collective behavior and in Section 3.3.2 we show that the orientation of water molecules can lag considerably behind the field reversal. As the aligning process requires finite time, the average dipole alignment of the system with the electric field decreases with increasing frequency. In the case where the electric field strength is $E_0 = 0.2\ V\ \text{Å}^{-1}$, the maximum alignment at the frequency ν = 200 GHz is approximately 60 % while it is below 35% at ν = 500 GHz. The lag is attributed to H-bonds impeding the (collective) response to the changing field. The faster the field is reversed, the fewer water molecules will follow the field and a larger fraction of those will reach only an incomplete reorientation.[55,56]

In addition to the reduction of the amplitude of the instantaneous average alignment (Figure 1), increasing the frequency also broadens the distribution of molecular alignments (see Figure 2). This means that the alignments of water molecules are less correlated to each other. We reinforce this observation in section 3.1.4. Figure 2 shows the distribution of molecular alignments as a

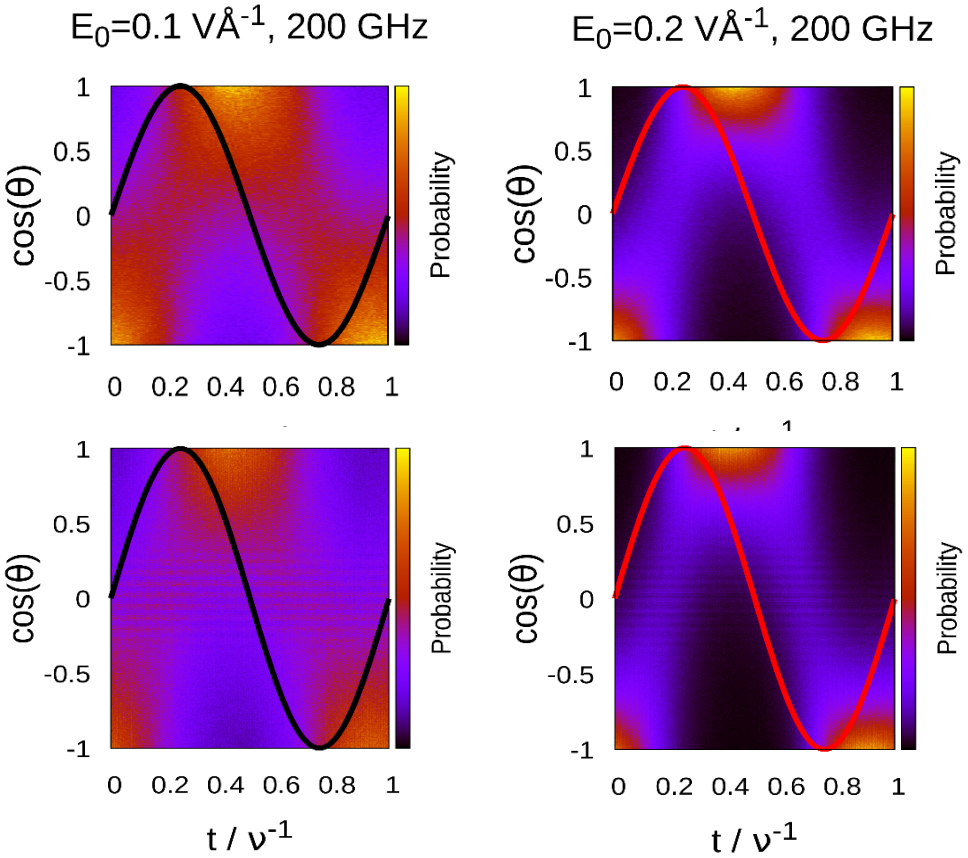

Figure 2. The angle distribution of dipole moments in SPC/E (top) and BK3(bottom) water relative to the direction of the alternating field as a function of time with yellow and black colors denoting maximal and minimal populations. The time in the x axis is normalized by the *E*-field period, . The solid lines are just sin(2πνt) showing the phase of the E-field. The distribution is narrower at , and we use different colors for the solid lines for better visibility.

function of time and compares the oscillations in the net polarization with those of the field. The intense color contrast on the right plot confirms that the distribution is much narrower under stronger E-field. The retardation of the alignment of water molecules is clear in this picture as the maximum alignment happens with a delay after the maximum E-field. The use of twice stronger AC field results in an only slightly accelerated polarization response.

The retardation of individual molecular alignment in relation to the E-field oscillations is due to molecules needing time to break hydrogen bonds. For instance, the upward dipole orientation peaks close to the half-period, $t=T/2$, when the field reverses to the negative (downward) direction. After the E-field is reversed, the molecules begin adapting to its new direction.

In Figure 3 we have plotted the time dependence of the (absolute) magnitude of the molecular dipole moment, $|\mu|$, for the polarizable water models. In each period, we observe two maxima and

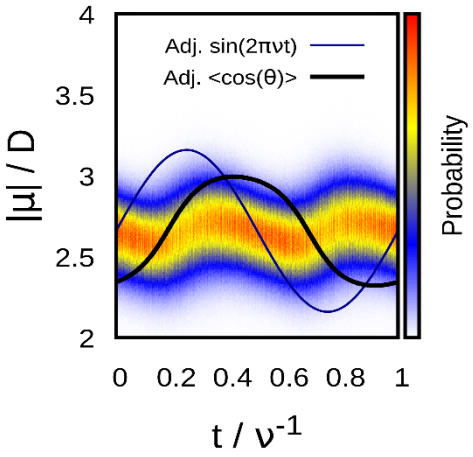

Figure 3. The distribution of the magnitude of the dipole moment, , in each period of the E-field. The thin solid line is the adjusted (scaled and shifted vertically) sinusoidal function representing the strength of the *E*-field, and the thick line is the adjusted average angle of the dipole moment in the direction of the E-field,

two minima for the magnitude of the dipole: At around $T/4$, the molecules are re-orienting from $-\hat{z}$ to $+\hat{z}$, so and $|\mu|$ reaches a minimum. At $T/2$, the water molecules have been under the positive E-field for about $T/2$, and $|\mu|$ peaks right before the *E*-field reverses. This maximum and minimum are repeated when the *E*-field is negative. So, the magnitude of the (absolute) dipole moment in each period of the E-field reaches two maxima, right after the *E*-field is at maximum in each direction, and two minima, right after the field reversals. The minimum of $|\mu|$ is equal to the zero *E*-field value ~2.64 D for BK3.[23] This figure also shows that, as expected, the response of the *magnitude* of the dipole moment to the applied field is faster than the polarization of the system due to the reorientation of the water molecules.

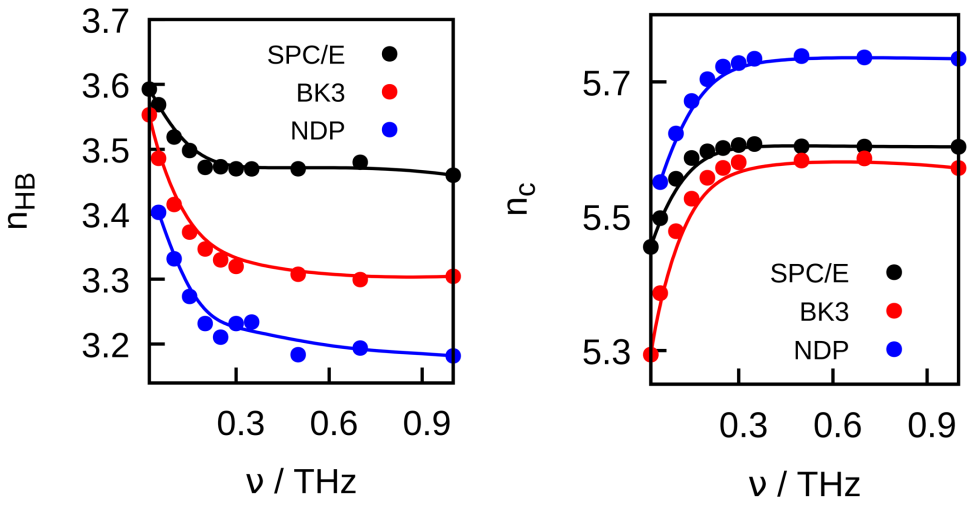

Figure 4. The number of H-bonds per water molecules (left) and the coordination number n_c, i.e. the number of neighboring molecules within the distance of 3.5 Å from the central molecule (right) under the different AC E-fields for SPC/E, BK3 and SWM4-NDP water models as functions of the frequency at $E_0 = 0.2\ V$ Å^{-1} where the effect of the *E*-field is strongest. Application of the AC E-fields decreases the number of H-bonds, but the percentage of the change under such high intensity and fast reversing alternating E-fields does not exceed 6% in any of the water models.

3.1.2. The number of hydrogen bonds

To characterize the hydrogen bonding behavior of water molecules under AC fields, we first focus on the average number of hydrogen bonds. We use the geometric H-bond criteria[44,57] that consider a pair of water molecules H-bonded if the distance of the donated hydrogen to the acceptor oxygen $d_{\mathrm{H}^*\cdots\mathrm{O}_a} < 2.4$ Å, and the hydrogen bond angle $\theta_{\mathrm{H}^*-\mathrm{O}^*\cdots\mathrm{O}_a} < 30°$.

Figure 4 shows only a minor reduction of the average number of hydrogen bonds under the alternating field.[36] The relative change depends on E_0 and the frequency, but the maximum change we observe is well below 10%. This relatively small change is observed even under an extremely strong field whose direction is reversed every $\frac{T_{500GHz}}{2} = 1\ ps$. At these conditions, around 60% of water molecules follow the *E*-field inversion. This is a very interesting observation since the water molecules cannot reorient without breaking at least some of their H-bonds,[57] and the conservation of the number of H-bonds under such fast reorientations requires that the H-bonds break and form at almost the rate of H-bond switching between distinct proton acceptors. In section 3.2, we measure hydrogen bond breaking and switching rate constants in AC-fields and show that they are close to each other.

In Figure 4, we have also plotted the average coordination number of water molecules, n_c, under the different alternating electric fields. Decreasing the number of H-bonds allows more molecules to be in proximity with each other, and the coordination number is slightly increased. Another way to describe n_c is as the summation of the H-bonded and non-H-bonded molecules inside the first coordination shell, which allows for the calculation of interstitial water molecules equal to the difference $n_c - n_{HB}$. This number increases with increasing E_0 and ν, but only by up to 6% and

this low increase does not affect the interstitial peak of oxygen triplet angle distribution shown in Figure 6.

The conservation of the number of hydrogen bonds and coordination number suggests that the tetrahedral structure of water is not changed substantially under the alternating *E*-fields. Very strong applied *E*-fields at high frequencies fail to disrupt the hydrogen bond structure.

According to Laage and Hynes,[43] the switching of a H-bond happens in a short time about $\approx 70\,fs$, which is much shorter than the waiting time between sequential switches, $\approx 3\,ps$, so increasing the number of switches under alternating E-fields does not influence the structure of water dramatically. We will assess this hypothesis in detail in the following sections, but before that, we look at additional criteria confirming the preservation of the structure of water.

3.1.3. Radial Distribution Functions and tetrahedral parameters

We have assessed the most important structural functions to see how they change with the field strength and frequency. The first function to observe is the radial distribution function, RDF or $g(r)$. Our results collected in Figure 5 reveal only minor changes in RDF under very strong, high frequency *E*-fields.[36] The positions of the peaks remain unchanged,[40] while the peaks and the minima are slightly less pronounced under stronger fields. Significant structural perturbations under such *E*-fields would, however, result in bigger reduction of the peaks, and possibly changed peak positions, which was not the case for any of the water models we consider.

Triplet Angle Distributions

An important measure of the tetrahedrality of the water network is the distribution of the oxygen triplet angle[38,39] (Fig 6). The distribution is calculated from the relation

$$P(\cos\theta_{\mathrm{OOO}}) = \frac{1}{N(n_i-2)}\left\langle \sum_{i=1}^{N}\sum_{j=1}^{n_i-1}\sum_{k=j+1}^{n_i}\delta\left(\cos\theta_{\mathrm{OOO}} - \frac{r_{ij}.r_{ik}}{|r_{ij}|\,|r_{ik}|}\right)\right\rangle \qquad [4]$$

where N is the total number of molecules, n_i is the number of nearest neighbors (within the first coordination shell) of molecule i, and r_{ij} and r_{ik} are vectors connecting the central molecule with its two nearest neighbors. This function measures the tetrahedrally of the system by calculating the angle between the vectors connecting the two nearest molecules with the central molecule.[58] The first peak of $O-O-O$ directly measures the tetrahedrality, and the second peak reflects the presence of interstitial, non-H-bonded water molecules. The change in the main peak below 10% which is indeed small under such strong and rapidly changing *E*-fields. Apparently, there is a less than a 10% change[59] in the tetrahedrality of water under an extreme *E*-field, $E_0 = 0.2\ V\text{Å}^{-1}$ and ν = 500 GHz, when compared to zero *E*-field.

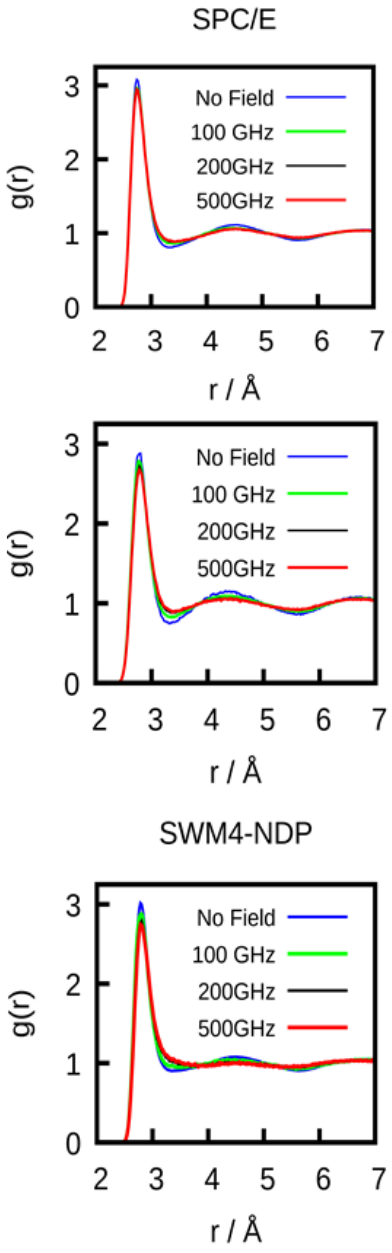

Figure 5. The radial distribution function of water under different AC field frequencies with a very strong *E*-field strength of 0.2 V Å^{-1} for SPC/E (top), BK3 (middle), and SWM4-NDP water models (bottom). The difference between the height and the position of the peaks for the different frequencies is small.

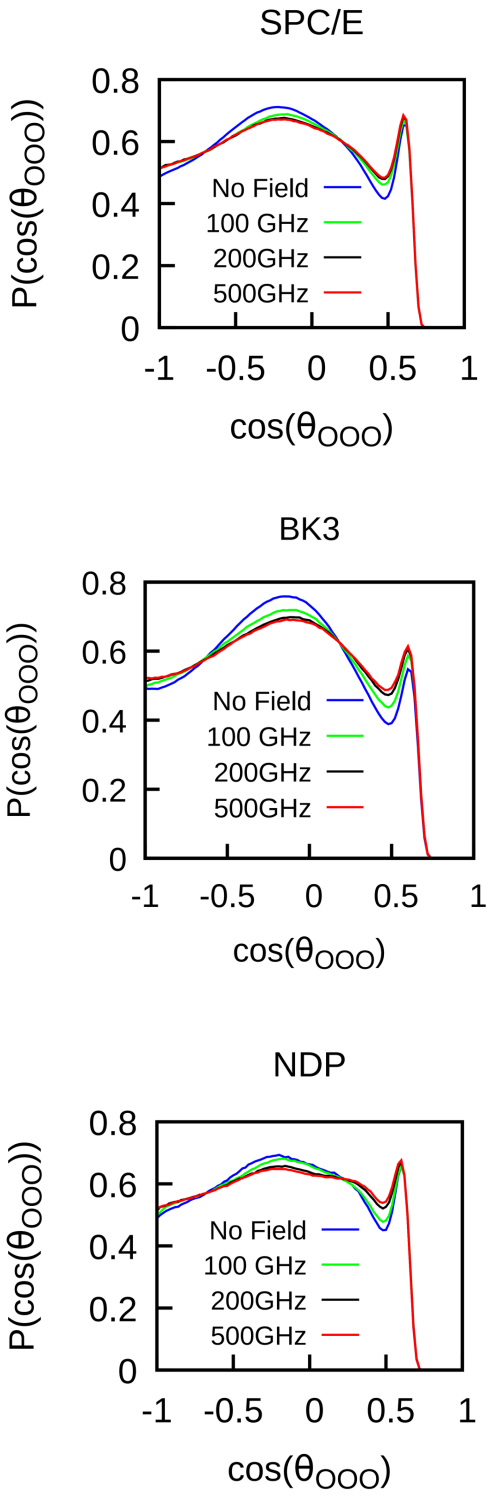

Figure 6. Oxygen triplet angle distribution, (Eq. 4), for water under different alternating E-field frequencies and $E_0 = 0.2V/\text{Å}$. The change in the main peak height remains below 10% which is relatively small considering the extreme strength and high frequencies of the field. The biggest change happens at 500 GHz, where Figure 1 reveals peak polarization near 35% of the saturated value showing that a substantial fraction of water molecules reverse their direction every 1ps.

3.1.4. Orientational Correlations

Periodic reorientation of water molecules the alternating *E*-field strongly depends on its H-bonding environment. In order to measure how entangled a water molecule is with the neighboring molecules[60], we look at the distance-dependent orientational correlations, $g_{dd}(r)$ expressed in terms of the water angle bisector vectors $\vec{d}$, [61,62]

$$g_{dd}(r) = \frac{\langle \vec{d}(0)\vec{d}(r) \rangle}{\langle d \rangle^2}. \qquad 5$$

The distance dependence of $g_{dd}(r)$ is illustrated in Figure 7, which shows that directional correlation between neighboring molecules decreases with increasing frequency of the *E*-field. The strongest angular correlation is observed at $\nu < 100\,GHz$ where the dynamics is comparatively slow. This confirms that during each cycle, the molecules have sufficient time to align with the *E*-field and with each other. We have also plotted the orientational correlation for a long distance, 10 Å: $g_{dd}(r \to \infty)$. At this distance, the apparent correlation reflects the overall alignment of the molecules with the field asymptotically approaching the square time average of the molecular orientation shown in Figure 1, $< \cos^2\theta >$. Like in other plots, we see a sharp decrease in the relative alignment of water molecules upon increasing the frequency, indicating that despite maintaining the structure, the long range order disappears under the rapidly reversing alternating fields. The above results prove that even strong AC-fields affect directional structure moderately while the radial structure remains mostly unchanged. [56,59]

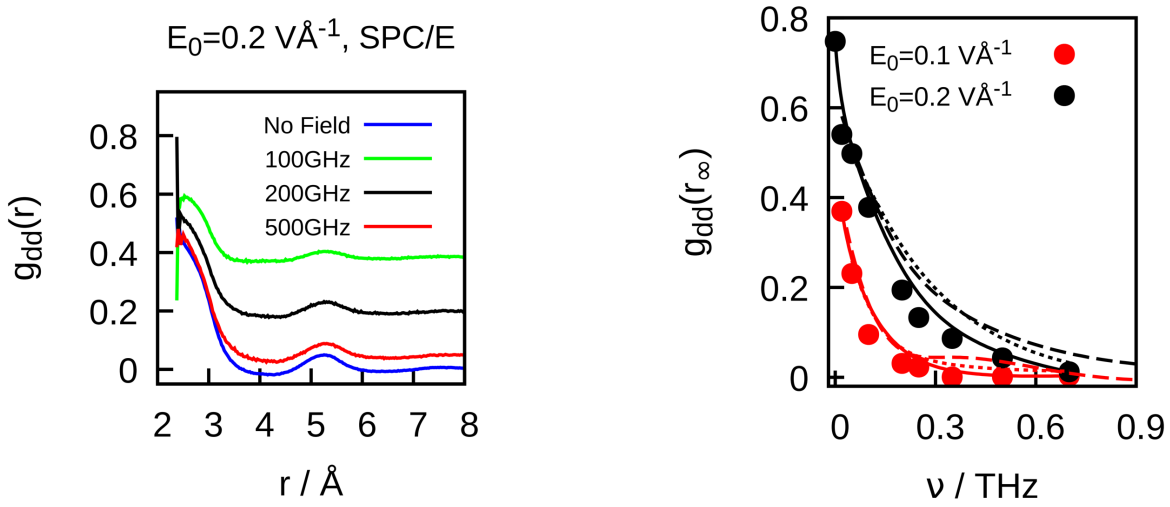

Figure 7. (Left) The directional correlation among of SPC/E water molecules, $g_{dd}(r)$, under $E_0 = 0.2\,\text{VÅ}^{-1}$ at different frequencies. The application of the *E*-field aligns the adjacent molecules, but increasing the frequency their directional correlations since adjacent molecules reorient with different rates controlled by different H-bonding state of the molecules. (Right) The limiting long-distance value of $g_{dd}(r)$ estimated at *r*=10 Å for SPC/E water molecules (solid lines). The same behaviour is observed with BK3 (dashed lines) and SWM4-NDP (dotted lines) models of water.

3.2. Hydrogen Bond kinetics

In this section, we characterize hydrogen bond dynamics under the influence of a wide range of alternating *E*-fields in terms of H-bonding rate constants. The classic model of hydrogen bonding, introduced by Luzar and Chandler[63] provides our first tool to measure the hydrogen bond lifetime[64,65]. In this model, the hydrogen bond correlation function, $c(t)$, is defined as the probability that an initially ($t = 0$) H-bonded pair of molecules is still bonded at time t, regardless of any breaking of H-bonds between these two times. The H-bond correlation function, c(t), can be defined as

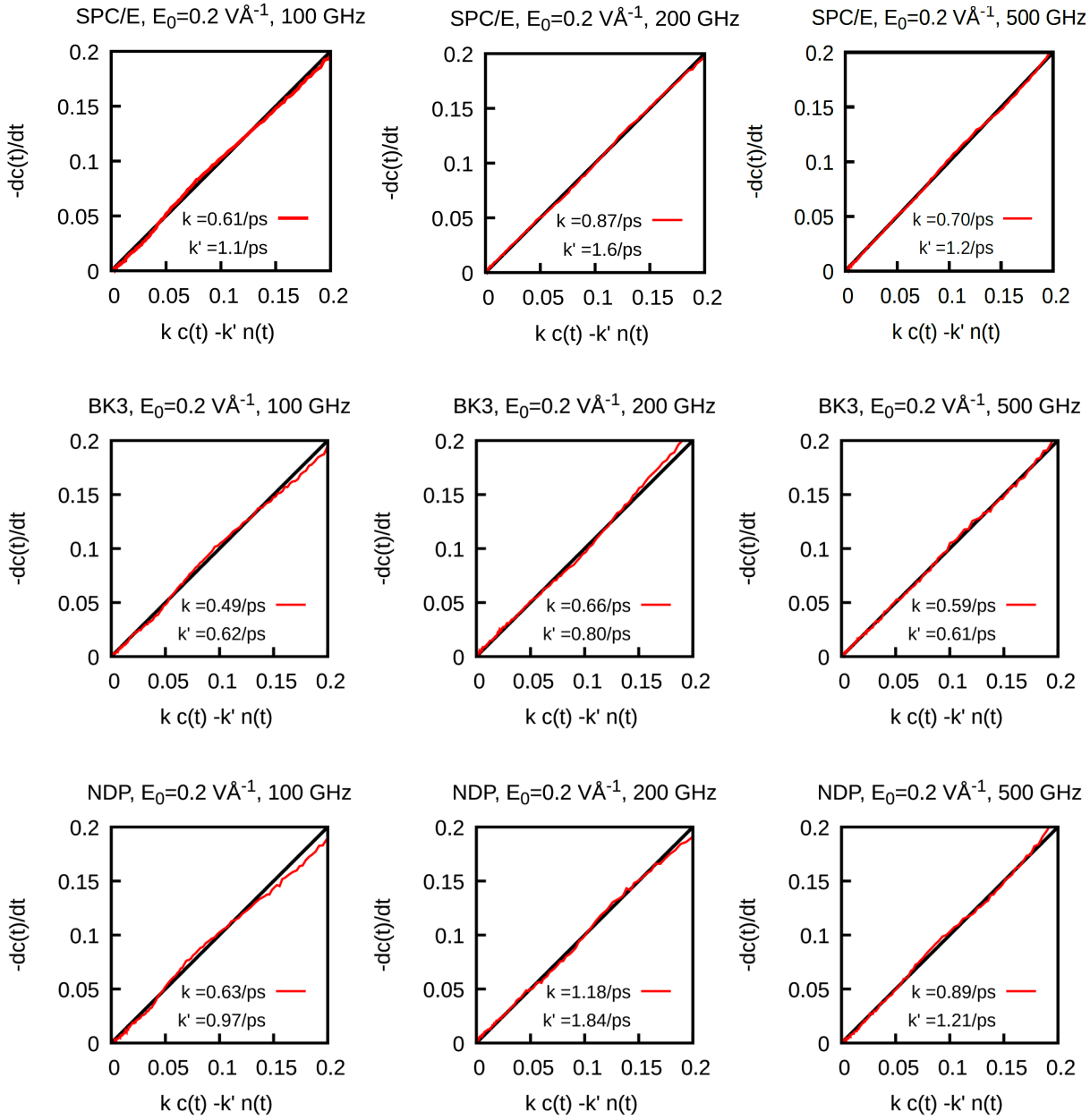

Figure 8. The correlation between the left and the right side of Eq. (8), and the optimal values of k and k'. The black line is a straight line with unit slope. We chose our highest E_0 to show that the phenomenological relation does not break even under such a strong *E*-field and rapid changes of the field direction.

$$c(t) = \frac{< h(t)h(0) >}{< h >} \quad [6]$$

where $h(t)$ is a dynamic variable, which is equal to 1 if a pair of molecules is H-bonded and zero otherwise. The probability of broken H-bond state is given as

$$n(t) = \frac{< h(0)[1 - h(t)]H(t) >}{< h >} \quad [7]$$

where $H = 1$ if the pair has not diffused apart, with the molecules still in the first coordination shell, and zero otherwise.

Assuming first order kinetics, $-\frac{d[\mathrm{A}]}{dt} = k[A] - k'[B]$, applied to the above time correlation functions,

$$k(t) = -\frac{dc(t)}{dt} = kc(t) - k'n(t). \quad [8]$$

we can calculate rate constants that satisfy eq.[8] by finding a pair of k and k' that best match the simulation data.

In the first step, we assess how this phenomenological model works under alternating *E*-fields. We have plotted the correlation functions along with the calculated rates for some E_0 and frequencies in Figure and we observe that under all *E*-fields this relation works very well, so the resulting rate constants continue to be reliable measures of the dynamics of H-bonding in alternating fields.

With a simple modification to the Luzar and Chandler model, we can calculate the rate of H-bond switching. We use a new phenomenological model to describe the elementary process of switching the H-bond acceptor. The two states are the first and the second H-bonded state of tagged hydrogen:

$$H^* \; donated \; to \; O_a \underset{k_s'}{\overset{k_s}{\rightleftharpoons}} H^* \; donated \; to \; O_b \quad [9]$$

where H* is the donated hydrogen attached to the donor oxygen, *O**, O_a is the first acceptor and O_b is the second acceptor molecule. We quantify the populations of above states with two correlation functions. The left side probability for tagged molecules is calculated by: $c_t(t) = \frac{<h_t(0)h_t(t)>}{<h_t(0)h_t(0)>}$ where h_t is 1 if the tagged hydrogen is donated to O_a and zero otherwise. The right side is the probability of switching $n_t(t) = \frac{<h_t(o)(1-h_t(0))h_t'(t)>}{<h_t>}$, where h_t' is 1 if the tagged hydrogen is H-bonded to O_b and zero otherwise. We distinguish between two probabilities based on when the tagged hydrogen switches its acceptor: the previous pair may stay in the first coordination shell of each other or leave. We distinguish between these two states as: $n_t^s(t) = \frac{<h_t(o)(1-h_t(0)(1-H(t))h_t'(t)>}{<h_t>}$ and $n_t^d(t) = \frac{<h_t(o)(1-h_t(0)H(t)h_t'(t)>}{<h_t>}$, where H is one if O_a is in the first coordination of O^* and zero otherwise. Analogous to the formalism for a tagged pair of molecules,

we can determine the best combination of k_s and k_s' or k_d and k_d' satisfying the following equations:

$$k_t(t) = -\frac{\mathrm{d}c_t(t)}{dt} = k_s c_t(t) - k_s' n_t^s(t), \quad [10]$$

and

$$k_t(t) = -\frac{\mathrm{d}c_t(t)}{dt} = k_d c_t(t) - k_d' n_t^d(t). \quad [11]$$

The rate constants k_s and k_d are closely related: $1/k_d$ is the time it takes a hydrogen to switch to another acceptor, and $1/k_s$ is the the time it takes a hydrogen to switch the acceptor *and* leave the first coordination shell. The switching process is complete when the previous pair separates beyond the first shell[66], so the H-bond switching rate is k_s and we only use k_d to estimate the time it takes for the previous acceptor to leave the first shell when the H-bond is switched: $\tau_r = 1/k_s - 1/k_d$.

In the next step, we study the trend of the hydrogen bond rate constants, k and k_s with changing frequencies under E-field strengths $E_0 = 0.1$ or $0.2\ V\text{Å}^{-1}$ for different water models. Results are collected in Figure 9 and Table 1. The H-bond breaking rate constant, k (Eq. 8) increases significantly with frequency until reaching ~ $200\ GHz$. There is maximum at around $200GHz$ for the H-bond breaking rate, k, (Figure 9), which will be discussed shortly. The trend of all the rate constants with frequency is the same: a steep increase until around $200GHz$ followed by a moderate decrease until $1\ THz$.

In Figure 9, we observe that the rate of H-bond breaking increases with the frequency of the alternating E-field until $\nu < 200\ GHz$. This means that for $\nu < 200\ GHz$, most molecules can respond to the oscillations of the E-field and reorient every cycle; increasing frequency therefore leads to accelerated switching and reforming of the H-bonds.

The trend, however, reverses when $\nu > 200\ GHz$: increasing the frequency decreases the H-bond breaking and switching rate constants. This means that the molecules can no longer respond to the faster E-field reversals by switching their H-bond ever faster. When $T/2$ is too short, the duration of the perturbing E-field is not long enough to force the molecules to break and switch their H-bonds, so a bigger fraction of the H-bonds survives through the field oscillation cycle. The probability of breaking the bond increases with the duration of the "*frustration time*" during which a bond is under strain due to a field-induced reorientation. The perturbation typically ends upon next field reversal and is hence limited to the half-period of the field oscillation, $t = T/2$. When $T/2$ becomes short in comparison to the mean bond-breaking time, the majority of H-bonds can survive the perturbation. Increasing the E-field frequency further only reduces the frustration time, thus decreasing any influence of the field on the average lifetime of H-bonds. [8,65]

Figure 10 shows the relation of $1/k_s$ and $T/2$: as long as $T/2$ is longer than $1/k_s$, increasing the frequency leads to accelerated H-bond dynamics. On the other hand, when $T/2$ is shorter than $1/k_s$, the higher the frequency the longer the average lifetime of the bonds. The frequency in which $1/k_s \sim T/2$ corresponds to around 150 GHz which means that increasing the frequency

above this value increases the chances of H-bonds surviving the perturbations due to the oscillatory field.

To sum up, the H-bonds have an inherent *response time* that is a characteristic time for water molecules to switch an H-bond. If external-field oscillations occur over shorter timescales, *i.e.* $\frac{T}{2} < \frac{1}{k_s}$, most molecules will not be able to respond to the oscillation and the original H-bonds will endure until the strain relaxes with the field reversal. On the balance, the shortened frustration time and better survival chance offset the increased frequency of perturbations in this regime, leading to increasing average lifetimes of hydrogen bond as the frequency is increased above ~200 GHz.[8,65] The precise value of the threshold frequency between the two regimes also depends on the strength of the field, E_0. As stronger *E*-field reduces the opportunities for bond reforming it generally results in lower $\frac{1}{k_s}$ (Figure 10). According to Figure 10, an increase of E_0 from 0.1 to 0.2 $V\text{Å}^{-1}$ leads to about 50% increase in the threshold frequency corresponding to the maximal k_s.

3.3. Diffusion

3.3.1. Translational Diffusion:

A direct consequence of accelerated H-bond kinetics in water under alternating *E*-fields is the change in translational and rotational diffusion.[21,51] In the previous section we showed that the application of the alternating E-field results in only a minor reduction of the number of hydrogen bonds. However, the dynamics of water molecules are much faster under alternating E-fields. In this section, we show that while each water molecule is still connected to the neighboring molecules, the faster H-bond dynamics results in a faster diffusion of water molecules.

We calculate the translational diffusion from the slope of the mean square displacement, MSD, over time between the 3-dimensional diffusion coefficient and the diffusion coefficient in the z direction have been plotted in Figure 11 for different E-fields, frequencies, and water models.

$$MSD = < (\vec{r}(t) - \vec{r}(0))^2 >. \qquad [12]$$

As expected, the diffusion coefficient is consistently higher for stronger *E*-field strengths across all measured frequencies. On the other hand, for the same E_0, the diffusion coefficient increases with frequency until around 200 GHz, and then slightly decreases.

In order to undergo a diffusive random step, a water molecule typically needs to switch an H-bond acceptor, leave the previous partner and transfer to the H-bonding region of a new acceptor.[67 68] The application of *E*-field influences these steps differently, but the main change is related to the H-bond lifetime. We showed in the previous section that there is a sharp increase in *k* with the

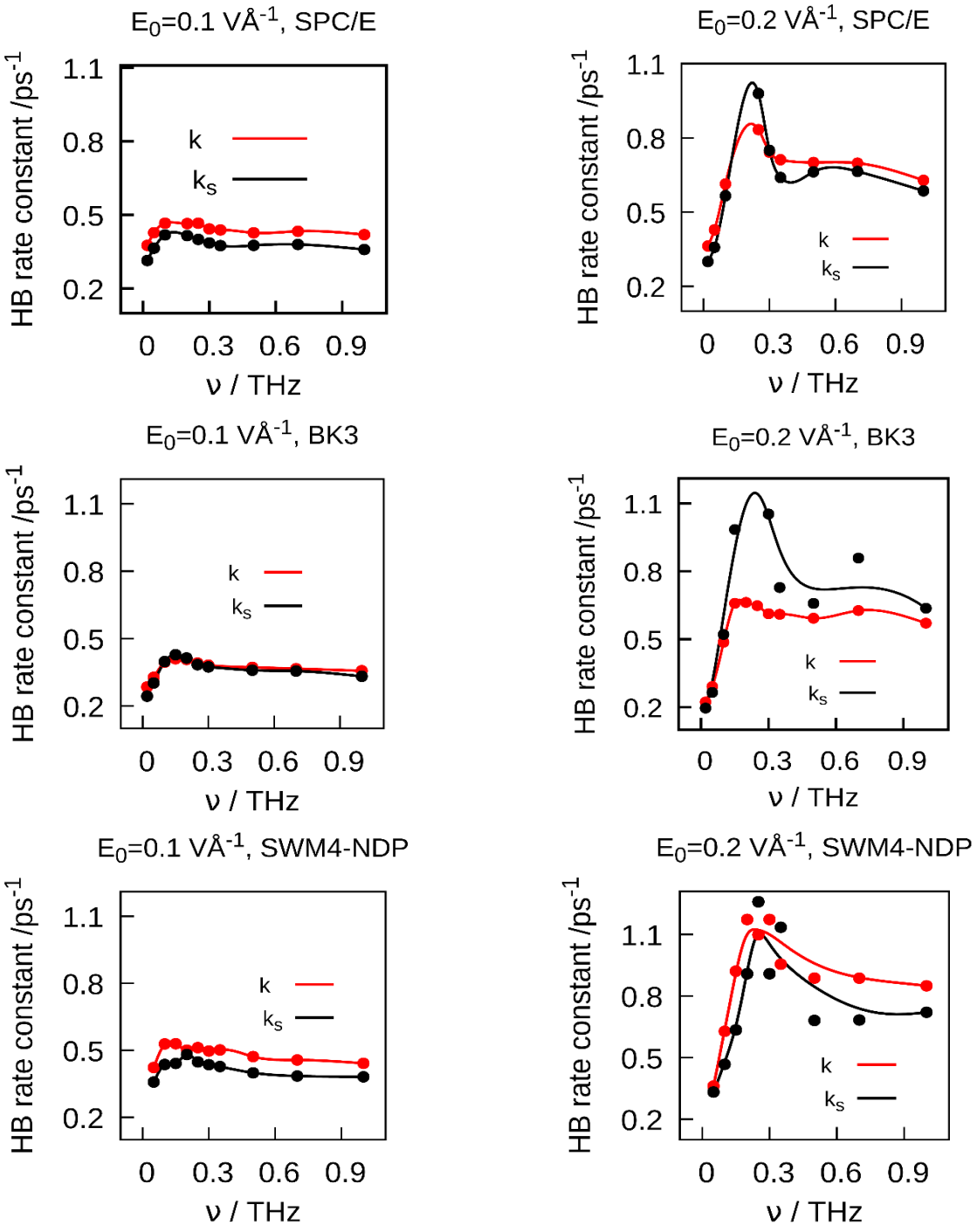

Figure 9. The different rates constants of hydrogen bonding from the methods that we presented in this report for two different strengths versus frequencies. All the rates constants are calculated from the correlation plots each with a maximum at the 200 GHz.

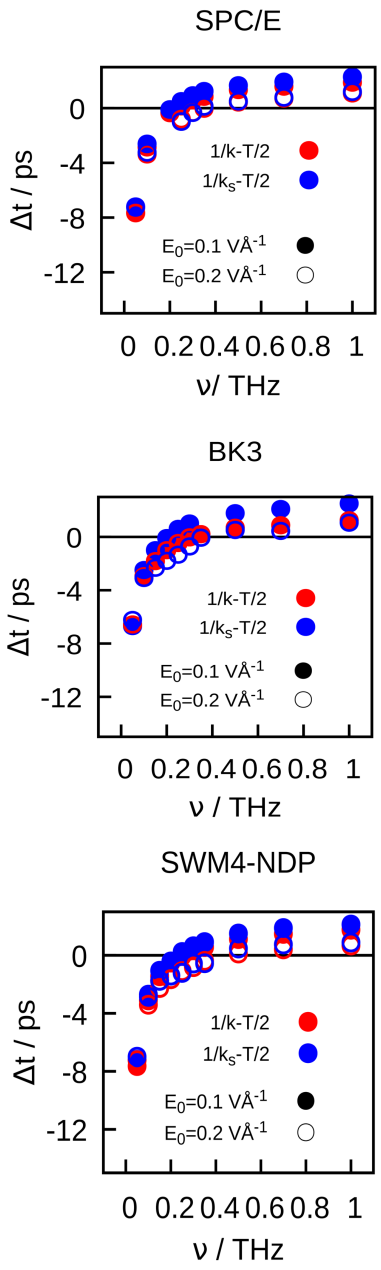

Figure 10. The relation of Δt, which is the time difference between alternating E-field half period time, $T/2$, and H-bond switching time, $1/k_s$, or H-bond breaking time $1/k$, and the E-field frequency. When the hydrogen bond breaking time is smaller than the half period, means $\Delta\, t < 0$, the higher E-field frequency results in a higher H-bond breaking rate, and we have faster dynamics. But when the half period is shorter than $1/k$, the water dynamics cannot follow the E-field reversal, and the breaking of hydrogen bond slows down with frequency (see Fig. 9).

frequency below ~200 GHz, and a moderate decrease thereafter. We observe almost the same trend in the translational diffusion coefficients shown in Figure 11.

Our diffusion results for SPC/E water are in excellent agreement with *ab-initio* simulations done by Futera and English[69] both qualitatively and quantitatively, indicating only weak independence on the choice of water model.

3.3.2. Rotational Diffusion

We calculate the rotational diffusion using the method introduced by Mazza *et al:* [70,71]

$$D_{R_p} = \lim_{t\to\infty} \frac{1}{4t} < \left|\overrightarrow{\phi_p}(t) - \overrightarrow{\phi_p}(0)\right| > \qquad (13)$$

Table 1. H-bond breaking rate constants, k and H-bond switching rate constants, k_s, for SPC/E water in the absence of the field or under AC fields of strengths $E_0 = 0.1$ or $0.2\ V\text{Å}^{-1}$ at three frequencies ν.

ν (GHz)	$\frac{T}{2}\ (ps)$	$E_0\ (V\text{Å}^{-1})$	$\frac{1}{k}(ps)$	$\frac{1}{k_s}(ps)$
-	-	no field	2.83	3.38
100	5	0.1	2.14	2.38
		0.2	1.63	1.77
200	2.5	0.1	2.14	2.40
		0.2	1.14	0.97
500	1	0.1	2.33	2.65
		0.2	1.43	1.51

where $\overrightarrow{\phi_p}(t)$ is the rotation vector of the dipole moment vector, p, using the right hand rule for rotation. The rotational diffusion, as well as translational diffusion, is intimately related to the H-bond dynamics.[72] The trend of the change of rotational diffusion with the frequency of the applied AC field illustrated in Figure 12 is very similar to the trends observed with the kinetics of breaking and switching of hydrogen bonds; when the H-bonds switch faster, the water molecules can travel and rotate at accelerated pace.[59]

In Figure 12, we also compare the rotational diffusion of the dipole moment, $\vec{p}$, of a molecule in the parallel and the perpendicular directions. When the dipole moment reorients from $+\hat{z}$ to $-\hat{z}$ or vise versa, we consider it as rotation parallel to the *E*-field, $R_{||}$, and when the dipole moment is rotating in a plane perpendicular to the E-field, *i. e.* in the xy plane, we term it a perpendicular rotation, $R_{\perp}$. All plots in Figure 12 reveal a pronounced anisotropy, with $R_{\parallel}$ generally exceeding $R_{\perp}$. The difference is explained by the effect of constantly changing z-component of the alternating E-field, which enhances up-down rotations. As the field is orthogonal to the xy plane, the field oscillations have no direct effect on $R_{\perp}$, although they will contribute indirectly through the

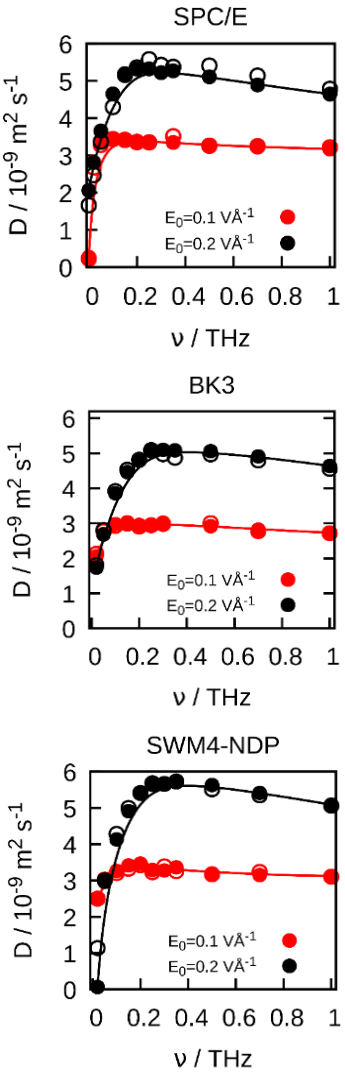

Figure 11. Translational diffusion for two E strengths for a range of frequencies for SPC/E (top left) BK3 (top right) and SWM4-NDP water model (bottom). The filled circles and lines are for overall 3D diffusion

increased occurrence of bond breaking events. The latter effect becomes insignificant at frequences ν exceeding the switching rate constant k_s. Consistent with this picture, the rotational diffusion of molecules inside $x-y$ plane, $R_{\perp}$, monotonically increases with the field frequency until around $\nu \sim 200\ GHz$ but becomes virtually independent of ν thereafter.

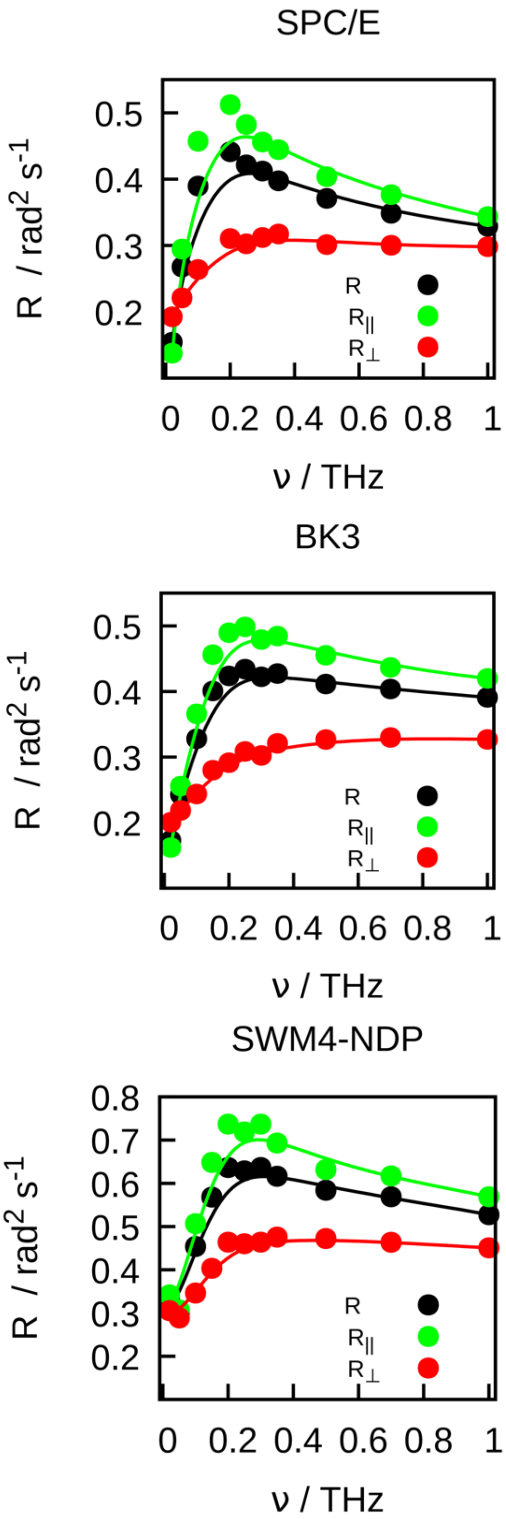

Figure 12. Rotational diffusion of the water dipole moment for $E_0 = 0.2\,V/\text{Å}$ in a range of frequencies for SPC/E water (top), BK3 water (middle), and SWM4-NDP water (bottom) models.The anisotropy of the rotation of the water molecules: $R_\perp$ and $R_\parallel$ is observable in all three water models.

4. Conclusion

We have studied the effect of high frequency alternating electric fields on the structure and dynamics of bulk water with special attention on hydrogen bonding. We show that when the field is strong enough and the frequency not too high, the average alignment of water molecules reverses after the field-direction change during each oscillation. The amplitude of the alignment, however, decreases with increasing frequency of the field.

Oxygen-oxygen radial distribution functions and oxygen-triplet angle distributions, which we monitored in a broad range of frequencies and multiple field strengths indicate only minor disruptions of the tetrahedral hydrogen-bond network under alternating electric fields. Our results, however, manifest a prominent, frequency dependent influence of the field on the dynamic properties of the system. Perpetual reorientations of water molecules following the oscillations of the field can accelerate the processes of bond-breaking and proton switching from one acceptor to another. The field effect is strong at intermediate frequencies (matching the timescales of elementary H-bonding events), while it weakens in both the low and high frequency limits. In the former extreme, the perturbations are too infrequent and in the latter, the duration of the oscillations is too short to induce a significant response. The frequency window where the AC-field has the largest impact is determined by the switching rate for the proton jumps between different proton acceptors. Because of the rapid replacement of broken bonds by new ones, even in this regime, there is at most a marginal increase in the population of broken bonds. We study the H-bond kinetics in the framework of the Luzar and Chandler tagged-pair model. The dynamics of H-bond switching is analyzed in a new version of the model that replaces pairs of tagged molecules by pairs of labeled protons and acceptors to determine correlation functions associated with the switching process. These calculations show both processes initially accelerate with the frequency of the *E*-field, reaching a maximum at around 200 GHz where the half-period of the AC-field is commensurate with a typical time of proton switching to another acceptor. Under higher frequencies, the effect of field oscillations becomes less significant allowing for a slow increase in the average H-bond lifetime and the time between the switching events. This behavior is attributed to the shortening of the dipoles' exposure to the reorienting field with a specified direction. When the duration of the *E*-field oscillations becomes short compared to the typical switching time, the H-bonds have a better chance to survive, or reform upon the next reversal of the field. Despite the increased frequency of reorientation attempts, the shortening of the 'frustration times' (inversely proportional to the frequency of oscillations) eventually results in slower H-bond dynamics and a return to the rates only slightly higher than in the absence of the field.

The above trend is reflected in the frequency dependence of observable properties like translational and rotational diffusion. As both processes depend on the kinetics of bond breaking and switching, they exhibit an analogous frequency dependence with the fastest diffusion coinciding with the extreme rates of H-bond breaking and partner-exchange processes. Irrespective of the field, these processes assume different rates in the interfacial region. A planned extension of our study concerns alternating field affects on the dynamics of interfacial water molecules where the tendency toward optimal hydrogen-bond coordination imposes additional orientation restrictions, potentially affecting the molecules' dynamic response to applied oscillatory fields. Analysis along these lines will be reported in the forthcoming work.

ACKNOWLEDGMENTS

While performing this work, M.S., N.O., and A.L. were supported by the National Science Foundation under Grant No. CHE-1800120 and S.Z., and D.B. were supported by the Office of Basic Energy Sciences, Chemical Sciences, Geosciences, and Biosciences Division of the U.S. Department of Energy (Grant No. DE-SC 0004406). We acknowledge the supercomputer time from Extreme Science and Engineering Discovery Environment (XSEDE), supported by NSF Grant No. OCI-1053575, and the National Energy Research Scientific Computing Center (NERSC), supported by the Office of Science of the U.S. Department of Energy (No. DEAC02-05CH11231).

References

[1]P. K. Nandi, N. J. English, Z. Futera, and A. Benedetto, Hydrogen-bond dynamics at the bio-water interface in hydrated proteins: A molecular-dynamics study, *Phys. Chem. Chem. Phys.* **19**, 318 (2016).

[2]Z. Futera and N. J. English, Electric-field effects on adsorbed-water structural and dynamical properties at rutile- and anatase-tio2 surfaces, *J. Phys. Chem. C* **120**, 19603 (2016).

[3]Winarto, E. Yamamoto, and K. Yasuoka, Water molecules in a carbon nanotube under an applied electric field at various temperatures and pressures, *Water* **9**, 1 (2017).

[4]S. D. Fried and S. G. Boxer, Measuring electric fields and noncovalent interactions using the vibrational stark effect, *Acc. Chem. Res.* **48**, 998 (2015).

[5]F. Saija, F. Aliotta, M. E. Fontanella, M. Pochylski, G. Salvato, C. Vasi, and R. C. Ponterio, Communication: An extended model of liquid bridging, *J. Chem. Phys.* **133**, 081104 (2010).

[6]M. R. Kemp and P. J. Fryer, Enhancement of diffusion through foods using alternating electric fields, *Innov. Food Sci. Emerg. Technol.* **8**, 143 (2007).

[7]P. Piyasena, C. Dussault, T. Koutchma, H. S. Ramaswamy, and G. B. Awuah, Radio frequency heating of foods: Principles, applications and related properties - a review, *Crit. Rev. Food Sci. Nutr.* **43**, 587 (2003).

[8]N. J. English, P. G. Kusalik, and S. A. Woods, Coupling of translational and rotational motion in chiral liquids in electromagnetic and circularly polarised electric fields, *J. Chem. Phys.* **136**, 094508 (2012).

[9]N. J. English, G. Y. Solomentsev, and P. O'Brien, Nonequilibrium molecular dynamics study of electric and low-frequency microwave fields on hen egg white lysozyme, *J. Chem. Phys.* **131**, 035106 (2009).

[10]N. J. English, D. C. Sorescu, and J. Karl Johnson, Effects of an external electromagnetic field on rutile tio2: A molecular dynamics study, *J. Phys. Chem. Solids* **67**, 1399 (2006).

[11]D. Bratko, C. D. Daub, K. Leung, and A. Luzar, Effect of field direction on electrowetting in a nanopore, *J. Am. Chem. Soc.* **129**, 2504 (2007).

[12]M. von Domaros, D. Bratko, B. Kirchner, and A. Luzar, Dynamics at a janus interface, *J. Phys. Chem. C* **117**, 4561 (2013).

[13]I. V. Stiopkin, C. Weeraman, P. A. Pieniazek, F. Y. Shalhout, J. L. Skinner, and A. V. Benderskii, Hydrogen bonding at the water surface revealed by isotopic dilution spectroscopy, *Nature* **474**, 192 (2011).

[14]N. Ojaghlou, H. V. Tafreshi, D. Bratko, and A. Luzar, Dynamical insights into the mechanism of a droplet detachment from a fiber, *Soft Matter* **14**, 8924 (2018).
[15]J. Su and H. Guo, Effect of nanochannel dimension on the transport of water molecules, *J. Phys. Chem. B* **116**, 5925 (2012).
[16]K. F. Rinne, S. Gekle, D. J. Bonthuis, and R. R. Netz, Nanoscale pumping of water by ac electric fields, *Nano Lett.* **12**, 1780 (2012).
[17]N. J. English and C. J. Waldron, Perspectives on external electric fields in molecular simulation: Progress, prospects and challenges, *Phys. Chem. Chem. Phys.* **17**, 12407 (2015).
[18]R. Kumar, J. R. Schmidt, and J. L. Skinner, Hydrogen bonding definitions and dynamics in liquid water, *J. Chem. Phys.* **126**, 204107 (2007).
[19]J. Teixeira, Recent experimental aspects of the structure and dynamics of liquid and supercooled water, *Mol. Phys.* **110**, 249 (2012).
[20]M. Chen, H. Y. Ko, R. C. Remsing, M. F. Calegari Andrade, B. Santra, Z. Sun, A. Selloni, R. Car, M. L. Klein, J. P. Perdew, and X. Wu, Ab initio theory and modeling of water, *Proc. Natl. Acad. Sci.* **114**, 10846 (2017).
[21]N. J. English and J. M. D. MacElroy, Molecular dynamics simulations of microwave heating of water, *J. Chem. Phys.* **118**, 1589 (2003).
[22]H. J. C. Berendsen, J. R. Grigera, and T. P. Straatsma, The missing term in effective pair potentials, *J. Phys. Chem.* **91**, 6269 (1987).
[23]P. T. Kiss and A. Baranyai, A systematic development of a polarizable potential of water, *J. Chem. Phys.* **138**, 204507 (2013).
[24]G. Lamoureux, E. Harder, I. V. Vorobyov, B. Roux, and A. D. MacKerell, A polarizable model of water for molecular dynamics simulations of biomolecules, *Chem. Phys. Lett.* **418**, 245 (2006).
[25]J. T. H. Guillaume Stirnemann, Damien Laage, Water hydrogen bond dynamics in aqueous solutions of amphiphiles, *J. Phys. Chem. B* **114**, 3052 (2010).
[26]S. Vaitheeswaran, J. C. Rasaiah, and G. Hummer, Electric field and temperature effects on water in the narrow nonpolar pores of carbon nanotubes, *J. Chem. Phys.* **121**, 7955 (2004).
[27]C. Merlet, B. Rotenberg, P. A. Madden, and M. Salanne, Computer simulations of ionic liquids at electrochemical interfaces, *Phys. Chem. Chem. Phys.* **15**, 15781 (2013).
[28]A. M. Saitta, F. Saija, and P. V. Giaquinta, Ab initio molecular dynamics study of dissociation of water under an electric field, *Phys. Rev. Lett.* **108**, 207801 (2012).
[29]E. M. Stuve, Ionization of water in interfacial electric fields: An electrochemical view, *Chem. Phys. Lett.* **519-520**, 1 (2012).
[30]J. D. Smith, R. J. Saykally, and P. L. Geissler, The effects of dissolved halide ions on hydrogen bonding in liquid water, *J. Am. Chem. Soc.* **129**, 13847 (2007).
[31]D. Bratko, B. Jonsson, and H. Wennerstrom, Electrical double-layer interactions with image charges, *Chem. Phys. Lett.* **128**, 449 (1986).
[32]J. Z. Wu, D. Bratko, and J. M. Prausnitz, Interaction between like-charged colloidal spheres in electrolyte solutions, *Proc. Natl. Acad. Sci.* **95**, 15169 (1998).
[33]D. Bratko and D. Dolar, Ellipsoidal model of poly-electrolyte solutions, *J. Chem. Phys.* **80**, 5782 (1984).
[34]J. D. Eaves and A. Tomakoff, Electric field fluctuations drive vibrational dephasing in water, *The Journal of Physical Chemistry A* **109**, 9424 (2005).
[35]D. Zong, H. Hu, Y. Duan, and Y. Sun, Viscosity of water under electric field: Anisotropy induced by redistribution of hydrogen bonds, *J. Phys. Chem. B* **120**, 4818 (2016).
[36]D. Li and G.-z. Jia, Dielectric properties of spc/e and tip4p under the static electric field and microwave field, *Physica A: Statistical Mechanics and its Applications* **449**, 348 (2016).

[37]I. M. Svishchev and P. G. Kusalik, Electrofreezing of liquid water: A microscopic perspective, *J. Am. Chem. Soc.* **118**, 649 (1996).
[38]R. D. Mountain and D. Thirumalai, Hydration for a series of hydrocarbons, *Proc. Natl. Acad. Sci.* **95**, 8436 (1998).
[39]C. D. Daub, K. Leung, and A. Luzar, Structure of aqueous solutions of monosodium glutamate, *J. Phys. Chem. B* **113**, 7687 (2009).
[40]W. Sun, Z. Chen, and S.-Y. Huang, Molecular dynamics simulation of liquid methanol under the influence of an external electric field, *Fluid Phase Equilib.* **238**, 20 (2005).
[41]A. Luzar and D. Chandler, Hydrogen-bond kinetics in liquid water, *Nature* **379**, 55 (1996).
[42]A. Luzar, Water hydrogen-bond dynamics close to hydrophobic and hydrophilic groups, *Faraday Discuss.* **103**, 29 (1996).
[43]D. Laage and J. T. Hynes, A molecular jump mechanism of water reorientation, *Science* **311**, 832 (2006).
[44]M. Shafiei, M. von Domaros, D. Bratko, and A. Luzar, Anisotropic structure and dynamics of water under static electric fields, *J. Chem. Phys.* **150**, 074505 (2019).
[45]J. A. Garate, N. J. English, and J. M. MacElroy, Static and alternating electric field and distance-dependent effects on carbon nanotube-assisted water self-diffusion across lipid membranes, *J. Chem. Phys.* **131**, 114508 (2009).
[46]M. Shafiei, Water dynamics and the effect of static and alternating electric fields, *Thesis, Virginia Commonwealth University, Richmond* (2018).
[47]S. Plimpton, Fast parallel algorithms for short-range molecular-dynamics, *J. Comput. Phys.* **117**, 1 (1995).
[48]B. Hess, C. Kutzner, D. van der Spoel, and E. Lindahl, Gromacs 4 algorithms for highly efficient, load-balanced, and scalable molecular simulation, *J. Chem. Theory Comput.* **4**, 435 (2008).
[49]B.-w.-m. M. Sega, https://github.com/Marcello-Sega/gromacs.
[50]M. P. Allen and D. J. Tildesley, *Computer Simulation of Liquids, Oxford University Press* (2017).
[51]N. J. English and J. M. D. MacElroy, Hydrogen bonding and molecular mobility in liquid water in external electromagnetic fields, *J. Chem. Phys.* **119**, 11806 (2003).
[52]D. J. Evans and B. L. Holian, The nose–hoover thermostat, *J. Chem. Phys.* **83**, 4069 (1985).
[53]G. Bussi, D. Donadio, and M. Parrinello, Canonical sampling through velocity rescaling, *J. Chem. Phys.* **126**, 014101 (2007).
[54]H. J. C. Berendsen, J. P. M. Postma, W. F. Van Gunsteren, A. DiNola, and J. R. Haak, Molecular dynamics with coupling to an external bath, *J. Chem. Phys.* **81**, 3684 (1984).
[55]S. De Luca, B. D. Todd, J. S. Hansen, and P. J. Daivis, Molecular dynamics study of nanoconfined water flow driven by rotating electric fields under realistic experimental conditions, *Langmuir* **30**, 3095 (2014).
[56]M. Tanaka and M. Sato, Microwave heating of water, ice, and saline solution: Molecular dynamics study, *J. Chem. Phys.* **126**, 034509 (2007).
[57]A. Luzar, Resolving the hydrogen bond dynamics conundrum, *J. Chem. Phys.* **113**, 10663 (2000).
[58]D. Bratko, C. D. Daub, and A. Luzar, Field-exposed water in a nanopore: Liquid or vapour?, *Phys. Chem. Chem. Phys.* **10**, 6807 (2008).
[59]P. K. Mishra, O. Vendrell, and R. Santra, Subpicosecond energy transfer from a highly intense thz pulse to water: A computational study based on the tip4p/2005 rigid-water-molecule model, *Phys. Rev. E* **93**, 032124 (2016).
[60]J. Kolafa and I. Nezbeda, Effect of short and long range forces on the structure of water. Ii. Orientational ordering and the dielectric, *Mol. Phys.* **98**, 1505 (2000).

[61]P. Mark and L. Nilsson, Structure and dynamics of liquid water with different long-range interaction truncation and temperature control methods in molecular dynamics simulations, *J. Comput. Chem.* **23**, 1211 (2002).
[62]H. J. C. Berendsen, D. van der Spoel, and R. van Drunen, Gromacs a message-passing parallel molecular dynamics implementation, *Comput. Phys. Commun.* **91**, 43 (1995).
[63]A. Luzar and D. Chandler, Structure and hydrogen bond dynamics of water–dimethyl sulfoxide mixtures by computer simulations, *J. Chem. Phys.* **98**, 8160 (1993).
[64]S. Floros, M. Liakopoulou-Kyriakides, K. Karatasos, and G. E. Papadopoulos, Frequency dependent non- thermal effects of oscillating electric fields in the microwave region on the properties of a solvated lysozyme system: A molecular dynamics study, *PLoS One* **12**, e0169505 (2017).
[65]R. Reale, N. J. English, P. Marracino, M. Liberti, and F. Apollonio, Dipolar response and hydrogen-bond kinetics in liquid water in square-wave time-varying electric fields, *Mol. Phys.* **112**, 1870 (2013).
[66]D. Laage and J. Hynes, On the molecular mechanism of water reorientation, *J. Phys. Chem. B* **112**, 14230 (2008).
[67]D. J. Bonthuis, S. Gekle, and R. R. Netz, Profile of the static permittivity tensor of water at interfaces: Consequences for capacitance, hydration interaction and ion adsorption, *Langmuir* **28**, 7679 (2012).
[68]J. Qvist, H. Schober, and B. Halle, Structural dynamics of supercooled water from quasielastic neutron scattering and molecular simulations, *J. Chem. Phys.* **134**, 144508 (2011).
[69]Z. Futera and N. J. English, Communication: Influence of external static and alternating electric fields on water from long-time non-equilibrium ab initio molecular dynamics, *J. Chem. Phys.* **147**, 031102 (2017).
[70]M. G. Mazza, N. Giovambattista, H. E. Stanley, and F. W. Starr, Connection of translational and rotational dynamical heterogeneities with the breakdown of the stokes-einstein and stokes-einstein-debye relations in water, *Phys. Rev. E* **76**, 031203 (2007).
[71]M. G. Mazza, N. Giovambattista, F. W. Starr, and H. E. Stanley, Relation between rotational and translational dynamic heterogeneities in water, *Phys. Rev. Lett.* **96**, 057803 (2006).
[72]H. J. Bakker, Y. L. A. Rezus, and R. L. A. Timmer, Molecular reorientation of liquid water studies with femtosecond midinfrared spectroscopy, *J. Phys. Chem. B* **112**, 11523 (2008).